Indian Journal of Pure & Applied Physics
Vol. 49, September 2011, pp. 619-626

Study of electronic and optical properties of Sc-, Y-, Ti-doped transparent conducting oxide

Yamini Sharma* & Pankaj Srivastava

Department of Physics, Feroze Gandhi College, Rae Bareli 229 001 (UP) India

*E-mail: yamini_2001@rediffmail.com

Received 18 October 2010; revised 12 May 2011; accepted 30 June 2011

Transparent conducting oxides have important applications as optoelectronic devices. First principles calculations have been performed to study the electronic and optical properties of Sc-, Y- and Ti-doped transparent conducting oxide (TCO) material CdO. The dielectric functions, absorption coefficients and transmittance spectra have been computed to study the effect of doping. The density of states have also been investigated to interpret the calculated optical spectra in terms of inter band transitions. The valence electron charge density is plotted to understand the redistribution of charges on introduction of transition metal ions. The electrical conductivity and Hall coefficient have also been calculated. The calculated band gap for pure CdO which is 0.51 eV increases significantly with doping. The band gaps for Sc-, Y- and Ti- doped CdO are 2.67, 2.83 and 2.53 eV, respectively, which are in good agreement with experimental measurements.

Keywords: Density functional theory, Transparent conducting oxides, Optical properties

1 Introduction

Pure and metal doped degenerate semiconductor oxides have been used in a wide range of optoelectronic applications like solar cells and optical communication. The optical and electrical properties can be controlled through doping with different types of metallic ions. Transparent conducting oxide (TCOs) like CdO has a relatively simple crystal structure with high carrier mobilities and conductivities which are enhanced with doping. CdO has been studied by photoemission spectroscopy and linear combination of atomic orbitals (LCAO) and many body perturbation theoretical methods[1-3]. Electronic structures of IIB-VIA binary compounds have been extensively studied by all electron local-orbitals Hartree-Fock method and also by quasi-particle band structure calculations. The optical and energy loss spectra have been obtained by means of spectroscopic ellipsometry[4,5]. The optical and electrical properties of CdO thin films at different temperatures have also been studied[6]. CdO thin films doped lightly by europium and samarium were prepared and studied by Dekhal[7,8]. Transport properties of gallium and indium doped thin films have been measured and studied by FP-LAPW method by Jin *et al*[9]. Doping of CdO system by Sc and Y has been investigated using the sX-LDA FLAPW scheme[10-12]. Some multi-component TCOs have also been studied by Medvedev[13,14]. Effect of doping on the band gap of *n*-type CdO has also been investigated[15]. Titanium doped CdO have been fabricated and characterized by studying the optical and electrical properties[16,17].

It is seen that doping of CdO by transition metal ions alters the optical properties like transmittance etc. However not much is known about the electronic structure of these doped TCO's. In the present study, electronic structure, optical and transport properties of Sc, Y and Ti doped CdO (CSO, CYO, CTO) using full potential linear augmented plane wave method (FP-LAPW), have been studied.

2 Computational Methodology

The density functional theory based full potential linear augmented plane wave method is a procedure for solving the Kohn-Sham equations (Eq. 1) for the ground state density, total energy, eigenvalues (energy bands) of a many-electron system by introducing a special basis set.

$$[-1/2\nabla^2 + V(r)]\phi_i^k = \varepsilon_i^k \phi_i^k \qquad \ldots(1)$$

The unit cell is divided into two parts (1) non-overlapping atomic spheres and (2) an interstitial region. Inside the atomic sphere t, of radius R_t, a linear combination of radial functions times the spherical harmonics $Y_{lm}(r)$ is used. Here u_l (r, E_l) is the regular solution of Schrödinger equation for energy E_l and for the spherical part of potential inside sphere *t*. The crystalline orbits can be written as:

$$\phi_{k_n} = \sum_{lm} [A_{lm}(k_n) u_l(E_l, r) + B_{lm}(k_n) u_l(E_{l,} r)] Y_{lm}(r) \quad \ldots(2)$$

In the interstitial region, a plane wave expansion is used:

$$\phi_{kn} = (1/\omega^{1/2}) e^{ik_n \cdot r} \quad \ldots(3)$$

Here $k_n = \mathbf{k} + \mathbf{K}_n$; $\mathbf{K}_n$ are the reciprocal lattice vectors and $\mathbf{k}$ is the wave vector inside the first Brillouin zone.

In its general form, the LAPW (APW+lo) method expands the potential as:

$$V(r) = \begin{cases} \sum_{LM} V_{LM}(r) Y_{LM}(\bar{r}) & r < R_\alpha \\ \sum_k V_k e^{iK \cdot r} & r \in I \end{cases} \quad \ldots(4)$$

The calculations here are performed using one of the most accurate methods, the Wien2k code in which no shape approximations are made[18]. The FP-LAPW including local orbits (lo) for the high lying semi core states. Within the density functional theory, the exchange and correlation are treated in the generalized gradient approximation (GGA) using the parameterization of Wu-Cohen[19]. Core states are treated fully relativistically while for the valence states, spin orbit interaction is added in the second variation step using the scalar-relativistic orbital as a basis. The density of states (DOS) has been calculated by using the modified tetrahedron method of Blochl *et al*[20].

Pure CdO is important as transparent conducting oxide, which exhibits transparency in the optical region. In order to gain better understanding, the frequency-dependent optical properties have been studied and calculated through the dielectric functions.

It is known that the optical response can be described by a complex frequency dependent dielectric function[21] $[\varepsilon(\omega)=\varepsilon_1(\omega)+i\varepsilon_2(\omega)]$. The imaginary part $\varepsilon_2(\omega)$, which arises from intra band and inter band transitions, depends on density of states (DOS) and the momentum matrix p and is calculated by considering all the possible transitions from occupied to unoccupied states (with fixed **k**-vectors) over the Brillouin zone (BZ). Mathematically, the

$$\varepsilon_2^{vv} = 8\pi^2 e^2 / m^2 \omega^2 \sum_{n}^{unocc} \sum_{n'}^{occ} \int_{BZ} \left| P_{nn'}^{v}(k) \right|^2 f_{kn}(1 - f_{kn'}) \times \delta(E_n^k - E_{n'}^k - \hbar\omega) \times d^3k / (2\pi)^3 \quad \ldots(5)$$

In the Eq. (5), m is mass of electron and Ω is the volume of unit cell. The function f_{kn} is the Fermi distribution and $|\mathbf{k}n\rangle$ is related to crystal wave functions corresponding to the n^{th} eigen value with crystal momentum k.

$$\varepsilon_2 = 1/N \sum_{i=1}^{N} \sigma_i^T \varepsilon_2(IBZ) \sigma_i \quad \ldots(6)$$

Real part of the dielectric function $\varepsilon_1(\omega)$ can be calculated from $\varepsilon_2(\omega)$ using the Kramers-Kronig relation as given below:

$$\varepsilon_1(\omega) = 1 + (2/\pi) P \int_0^\infty \varepsilon_2(\omega') \omega' d\omega' / (\omega'^2 - \omega^2) \quad \ldots(7)$$

where P implies the principal value of the integral. The reflectance can be calculated using the relation:

$$R^{vv}(\omega) = \left| (\varepsilon(\omega)^{1/2} - 1) / (\varepsilon(\omega)^{1/2} + 1) \right|^2 \quad \ldots(8)$$

The absorption coefficient $\alpha(\omega)$ can also be deduced from the dielectric function as given below:

$$\alpha(\omega) = 2\omega \left(\left[\varepsilon_1^2(\omega) + \varepsilon_2^2(\omega) \right]^{1/2} - \varepsilon_1(\omega) \right/ 2 \left. \right)^{1/2} \quad \ldots(9)$$

The semi classic transport coefficients are calculated using program Boltztrap[22] interfaced with Wien2k. The calculation relies on a Fourier expansion of the band energies where the space group symmetry is maintained by using star functions. Properties such as conductivity, Hall and Seebeck coefficients can be obtained from the Boltzmann theory.

In presence of an electric and magnetic field and a thermal gradient, the electric current, j, can be written in terms of the conductivity tensors:

$$j_i = \sigma_{ij} E_j + \sigma_{ijk} E_j B_k + v_{ij} \nabla_j T + \ldots\ldots \quad \ldots(10)$$

The conductivity tensors can be obtained:

$$\sigma_{\alpha\beta}(\mathbf{i}, \mathbf{k}) = e^2 \tau_{i,k} v_\alpha(\mathbf{i}, \mathbf{k}) v_\beta(\mathbf{i}, \mathbf{k}) \quad \ldots(11)$$

where τ is the relaxation time which depends on the band index **i** and **k** vector direction, and v is the group velocity.

The density of states energy projected conductivity tensor[11] is given in terms of Eq. (11) as:

$$\sigma_{\alpha\beta}(\varepsilon) = i/N \sum_{i,k} \sigma_{\alpha\beta}(i,k) \delta(\varepsilon - \varepsilon_{ik}) / d\varepsilon \quad \ldots(12)$$

where N is the number of k-points sampled. The transport tensor[10] Eq. (10) can be calculated from the conductivity distributions:

$$\sigma_{\alpha\beta}(T,\mu) = 1/N \int \sigma_{\alpha\beta}(\varepsilon)[\partial f_{\mu}(T;\varepsilon)/d\varepsilon]d\varepsilon \qquad \ldots(13)$$

The Hall coefficient can easily be calculated:

$$R_{ijk} = E_j^{ind} / j_i^{appl} B_k^{appl} = (\sigma^{-1})_{\alpha j} : \sigma_{\alpha\beta\kappa}(\sigma^{-1})_{\alpha\beta} \qquad \ldots(14)$$

CdO has the Fm3m crystal structure with space group 225 and lattice parameter[23] a=4.6953 Å. In the unit cell of CdO, there are two non-equivalent Cd atoms and two kinds of O atoms. A 2×2×1 super cell is constructed to obtain 32 atoms in the unit cell. Cadmium ion is replaced by transition metal ions scandium, yttrium and titanium to get the 1.6% doped materials. The lattice parameters of transparent conducting crystals do not show any change on doping. The $R_{MT}K_{max}$ was set equal to 7 for the convergence parameter for which the calculation stabilizes and energy convergence is achieved. Here R_{MT} is the smallest Muffin-tin radius and K_{max} is the cut-off wave vector of the plane-wave. The maximum radial expansion l_{max} is set to be 10. A mesh with 47 **k**-points in the irreducible Brillouin zone (IBZ) was used for CdO as well as Sc-, Y- and Ti- doped CdO. The energy cut-off between the core and valence states was set at −6.0 Ry.

3 Results and Discussion

Cadmium oxide adopts a face-centered-cubic rock salt structure based on octahedral coordination around Cd. Due to its high electrical conductivity and transparency in the optical region, CdO has been the subject of study for some time. However, in an effort to enhance these properties for more applications, the doping of CdO with transition metal ions with ionic radii smaller than Cd^{2+} has been studied. The effect of tuning of the electronic structure through doping of 1.6 % atom of transition metal ions, Sc-, Y- and Ti of differing ionic radii is clearly observed from the calculated optical properties. The radii for Sc^{2+}, Y^{2+} and Ti^{3+} are 0.745, 0.9 and 0.605 Å, respectively, which are relatively smaller than the ionic radius of Cd^{2+} i.e. 1.09 Å In the FP-LAPW method the optical properties are computed through the dielectric functions using Eq. (5). The imaginary part $\varepsilon_2(\omega)$ depends on the joint density of states and the momentum matrix elements. The Kramers-Kronig relations is used to obtain the real part $\varepsilon_1(\omega)$ from the imaginary $\varepsilon_2(\omega) = \varepsilon_{xx} + \varepsilon_{yy} + \varepsilon_{zz}/3$.

In Fig. 1(a), the average real or static part of the dielectric functions for pure and doped CdO for the energy range 0-12 eV, has been presented. The most important quantity is the zero frequency limit ε(0), which is the electronic part that strongly depends on the band gap. The refractive index **n** measured at frequencies above the lattice vibrational frequency is also related to ε(0) by the relation $n(0) = \sqrt{\mathrm{Re}\,\varepsilon(0)}$. The calculated refractive indices are 2.68, 2.82, 2.28 and 3.51 for CdO, CSO, CYO and CTO, respectively (Table 1). The refractive index of Ti doped-CdO shows anomalous behaviour. The calculated refractive index for CdO agrees very well with the experimental value[26] of 2.5. The refractive indices for the doped samples are not available for comparison.

In Fig. 1(b), the imaginary part of the average dielectric function for pure and doped CdO is presented for the energy range 0-12 eV. The general shapes of the dielectric functions show similarities with systematic trends excepting Ti-doped CdO. For pure CdO which has a cubic phase, the dynamic dielectric constants ε_{xx}, ε_{yy} and ε_{zz} do not exhibit any directional anisotropy. The calculated longitudinal and transverse dielectric functions are almost identical within a difference of about 1% indicating that the CdO and doped CdO do not exhibit directional anisotropy. The prominent energy peaks in $\varepsilon_2(\omega)$ for CdO appear at 4.61, 5.94 and 7.85 eV, for Sc-CdO the peaks are found at 4.02, 4.34, 6.11 and 8.10 eV, for Y-CdO the prominent peaks are located at 3.11, 3.70, 4.46, 5.17 and 6.36 eV, and for Ti-CdO the peaks appear at 0.98 and 4.22 eV. These energy peaks can

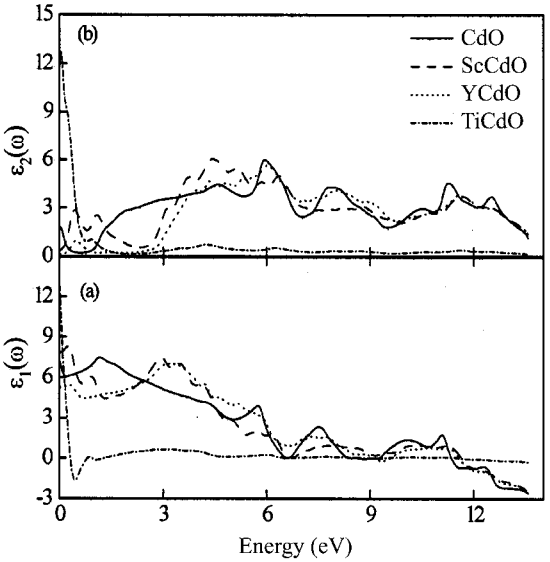

Fig. 1 — Real and Imaginary dielectric functions for CdO and Sc-, Y-, Ti-doped CdO

Table 1 — Electronic, optical and thermoelectric properties Sc-, Y-, Ti-doped CdO

Properties		CdO	Sc-CdO	Y-CdO	Ti-CdO
E_g (eV)	This Work	0.51	2.67	2.93	2.53
	Previous Work	2.4 [6] Expt. 1.0 [11] sX-LDA 1.61 [1] LCAO 6.56 [4] HF 0.5 [3] FP-LAPW	3.00 [12] Expt.	3.1 [11] Expt.	2.6 [16] Expt.
Refractive Index (n)		2.68 2.5 [26]	2.82	2.28	3.51
Hall Coefficient (R_H)(m^3/C)(10^{-10})		−3.81	−0.134	−0.120	−0.124
Electrical Conductivity (σ) ($\Omega^{-1}m^{-1}$)(10^4)		3.966 5.3 [6] Expt.	16.68	20.03	3.57

be related to optical transitions, which are intra and inter band transitions from valence bands to the conduction bands. From the s, p and d projected densities of states of Cd, O, Sc, Y and Ti in CdO, CSO, CYO and CTO, we can analyse the origins of the absorption peaks.

The total and partial density of states (DOS) for CdO, CSO, CYO and CTO computed by the FP-LAPW method are shown in Figs 2-5. The energy states can be divided in three main groups. It is seen that doping with ions of varying radii dramatically alters the energy states of CdO due to extensive mixing and hybridization of orbitals.

The main features of the density of states are presented here:

(i) The computed density of states for pure CdO is shown in Fig. 2. In the valence band, the s and p-states of Cd are found in the lowermost energy range –7.39 to –5.75 eV. In the valence band maximum (VBM) in the energy range –3.78 to 0 eV, the 2p-states of O contribute mainly, with intermixing of s, p and d states of Cd. In the conduction band (CB), hybridized 5s and 5p states of Cd are spread from 0.51 to 6.04 eV. In the topmost panel in Fig. 2, from the calculated partial density of 2p states of O, the peak positions at –0.34, –1.28, –3.35 eV in the valence band and peaks at 4.2, 5.76 and 6.89 and 8.23 eV in the CB can be seen. The calculated partial density of 2p-states for oxygen[19] using the latest GGA are in good agreement with soft X-ray emission spectroscopy (XES) peaks and X-ray absorption spectroscopy (XAS) O k-edge peaks[2].

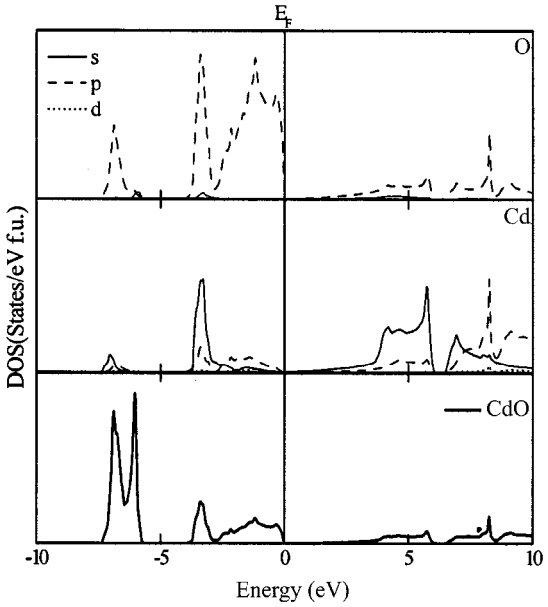

Fig. 2 — Partial and total density of states (PDOS and TDOS) of CdO

(ii) The energy states of the dopant ions hybridize with states of Cd and O giving rise to very interesting properties. The partial and total density of states for the doped-CdO are shown in Figs 3-5. The energy states for CSO, CYO and CTO also appear in three main groups.

For Sc-doped CdO, the lowermost energy states appear from –7.33 to –5.68 eV as shown in Fig. 3. These states consist of 2p-states of O and s and p-states of Cd and Sc. In the valence band region, the energy states are available from –4.07 eV to E_F. Due

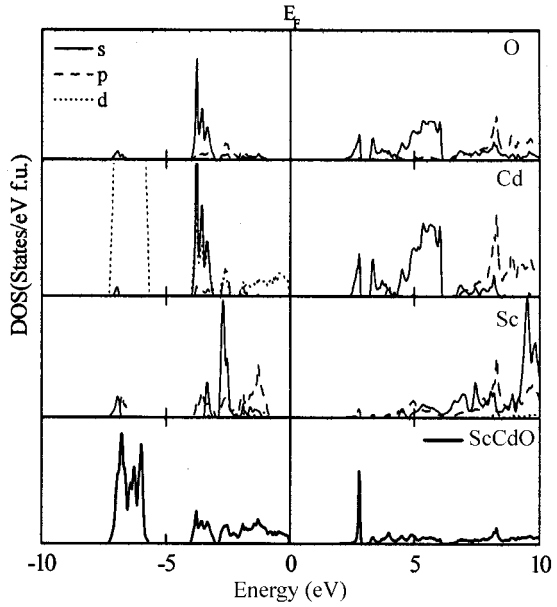

Fig. 3 — Partial and total density of states (PDOS and TDOS) of Sc-doped CdO (CSO)

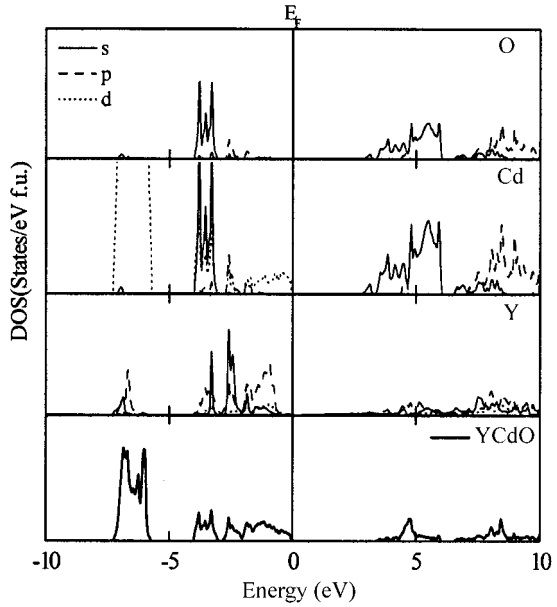

Fig. 4 — Partial and total density of states (PDOS and TDOS) of Y-doped CdO (CYO)

to the replacement of Cd ion by the dopant Sc^{3+} ion, the additional d-states of Sc^{3+} ions repel the d-states of Cd^{2+} ions to lower energy states. Thus, the d and p-states of Cd^{2+} are pushed downwards substantially in the VBM. The Cd d-states which contribute up to –3.78 eV for pure CdO, extend to –7.33 eV on doping CdO by Sc. Additional p-states of dopant ions contribute from –0.61 to –4.07 eV.

In the conduction band (CB), there is substantial mixing of s, p and d orbitals of dopant and Cd atoms,

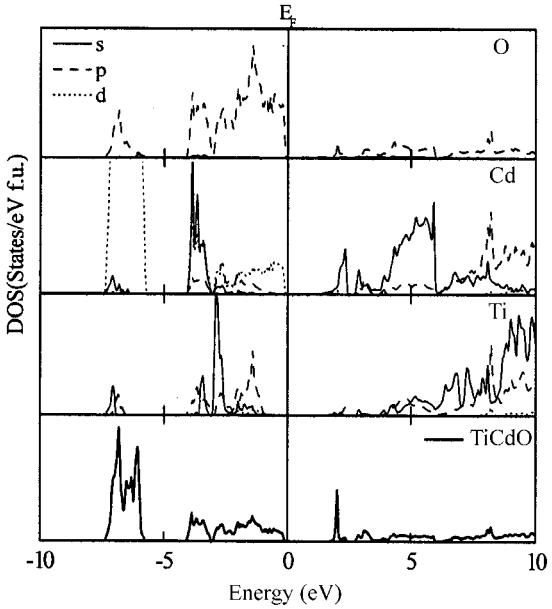

Fig. 5 — Partial and total density of states (PDOS and TDOS) of Ti-doped CdO (CTO)

leading to hybridized states. Due to additional d-states of dopant ion, the lowest states in the conduction band are blocked, leading to well known Burstien-Moss effect[24,25]. This causes the band gap to widen. Further, the prominent s-states of pure Cd in the CB shows a shift towards the Fermi energy level on doping.

From Figs (4 and 5), it is seen that the energy states for Y-doped CdO and Ti-doped CdO are similarly dispersed. For Y-CdO, the lowermost states appear from –7.39 to –5.75 eV, and the valence band states are found from –4.03 eV to E_F. Similarly for Ti-CdO, the lowermost states appear from –7.42 to –5.73 eV, and the valence band states are found from –4.1 eV to E_F. The s, p and d orbitals in the conduction band are very similar to the DOS of Sc-doped CdO.

From the DOS in Figs 3-5, it is observed that the 4s states of the dopant ion are found to lie high up in the conduction band. Due to smaller size of dopant ion, the outershell s-states of Sc, Y and Ti are not energetically comparable to s-state of Cd. Hence due to the difference in energy the dopant s-states do not hybridize with 5s states of Cd. The d-states of Sc/Y/Ti hybridize only with the p-orbitals of nearest oxygen neighbours. This can also be observed in the electron valence charge density plots in Fig. 6. Here, it is seen that the dopant ion has replaced Cd ion.

The electronic structure has a large impact on the optical properties and the analysis of the absorption spectra of Sc, Y and Ti doped CdO (CSO, CYO, CTO) has been carried out. In Fig. 7, the absorption

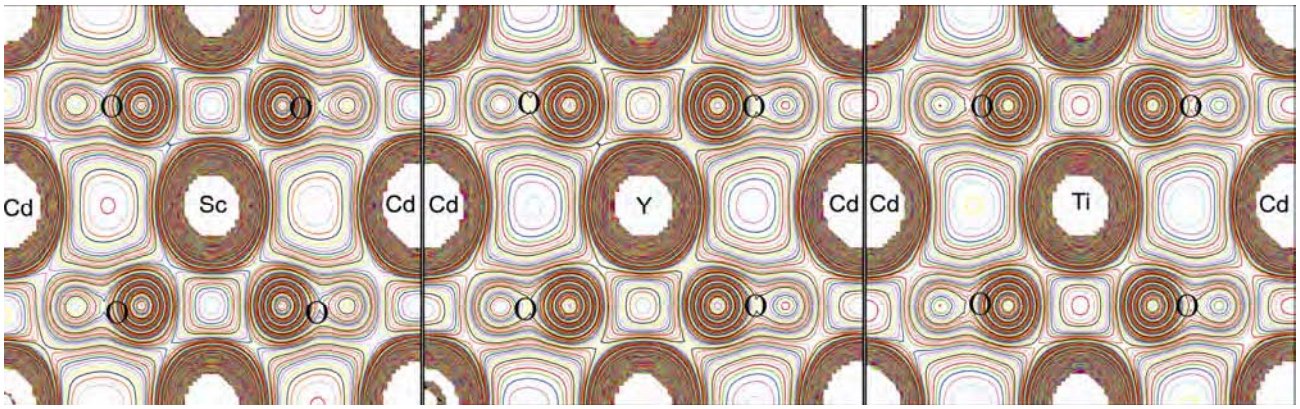

Fig. 6 — 2D electron valence charge density of Sc-CdO, Y-CdO and Ti-CdO in 110 plane

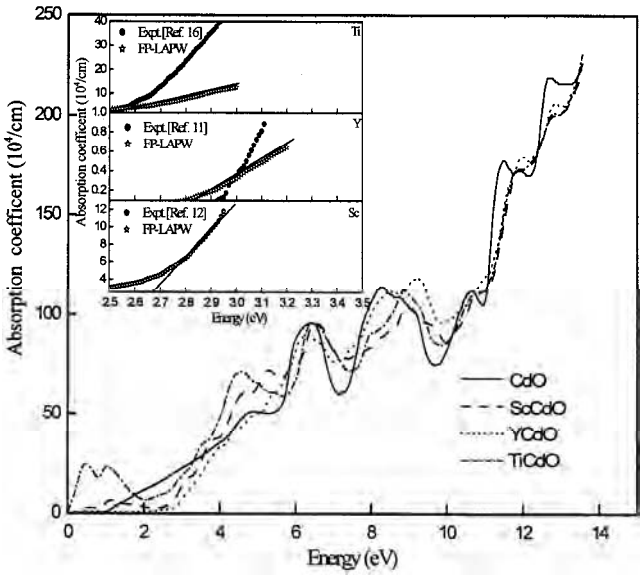

Fig. 7 — Absorption coefficient α(ω) vs energy (eV) of CdO, Sc-CdO, Y-CdO and Ti-CdO. Inset shows the extrapolated linear portion of experimental absorption spectra with calculated absorption coefficients by FP-LAPW method

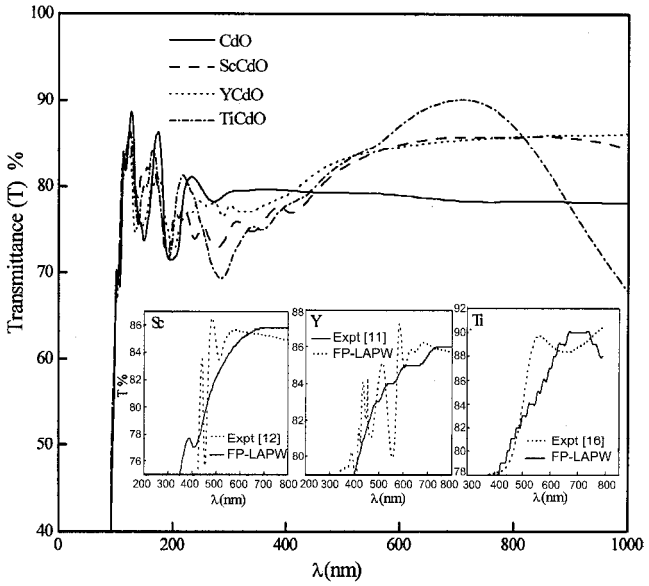

Fig. 8 — Transmission spectra (T %) versus wavelength (λ) (nm) of CdO, Sc-CdO, Y-CdO and Ti-CdO. Inset shows the experimental transmittance spectra with calculated transmittance by FP-LAPW method

coefficient α(ω) is computed according to Eq. (9). The absorption is plotted for photon energies in the range 0-14 eV. The prominent peaks for CdO occur at 4.81, 6.43, 8.26, 11.5 and 12.65 eV. For Sc-doped CdO, the peak values occur at 4.52, 6.5, 8.86 and 11.83 eV. In the case of Y-doped CdO, the peaks are located at higher energies corresponding to 6.2, 8.48, 9.21, 11.95 and 12.83 eV, whereas Ti-doped CdO shows peaks at lower energy corresponding to 0.44, 1.08 eV, the higher energy peaks appear at 4.47, 6.30, 9.20 and 11.96 eV.

These peaks can be interpreted as inter band transitions from O p→s-states, Cd s→p-states. All these inter band transitions are allowed by dipole transitions condition $\Delta l = \pm 1$. From the computed DOS, it is seen that due to introduction of extra states in CdO, the large BM shift causes the band gap to increase and inter band transitions from the valence band to the conduction band occur for higher energy. The higher energy peaks indicate that inter band transitions in the visible region are absent, which verify that these materials are optically transparent. Some lower energies peaks are observed for Sc and Ti-doped CdO which correspond to intra band transitions.

In the optical regions between 1.6 to 3.1 eV, there is very low absorption ~ 10×10^{4} /cm for CdO, which supports the direct band gap nature of the semiconductor. The Sc and Y-doped CdO also show low absorption, except for Ti doped CdO, which

shows some anomalous behaviour since some weak absorption peaks in the IR region are found.

The plot of $\alpha(\omega)$ versus $h\nu$ shows a linear behaviour in the optical region which also implies direct transitions. The straight portion is extrapolated to the energy axis at $\alpha = 0$, which gives the band gap of 2.67, 2.83 and 2.53 eV for Sc-, Y- and Ti-doped CdO, respectively. The calculated and experimental band gap are presented in Table 1. The band gap shows increasing trend with increasing ionic radii i.e. Y>Sc>Ti. Larger ionic radius dopant results in a larger optical band gap. The FP-LAPW calculated absorption coefficient shows close agreement with experiment.

Optical properties are mainly obtained by measuring transmittance spectra in the UV-Vis-NIR regions. Experiments on the optical reflectivity and transmittance are used to determine the dielectric constant of the solid, which is related to the band structure. The calculated transmittance is obtained from the reflectance $R(\omega)$ using Eq. (8). The transmittance spectra for CdO and doped CdO are shown in Fig. 8 for wavelengths in the range 0-1000 nm. For pure CdO about 75-80% transmittance is observed in the entire optical region in the range 400-700 nm. Sc- and Y-dopedCdO, show an average enhanced transmittance of 80-85% in the optical region. The transmittance of Ti-doped CdO shows an anomalous behaviour and has nearly 90% transmittance for the 698 nm wavelength. The transmittance of pure and doped CdO for shorter wavelengths in UV region shows an oscillatory behaviour. In the inset, the calculated transmittance is compared with experimental transmittance[12] for 1.2% atom Sc-CdO and 1.5% atom[11] Y-CdO. The average transmittance at 550 nm is ~85% for both the materials. The inset also shows experimental curve[16,17] for 2.5% atom Ti-doped CdO. Here, the experimentally measured transparency lies in the range 85-90% at 550 nm in the visible region. The FP-LAPW calculated transmittance thus shows close agreement with experiment.

From the calculated optical properties, it is found that the transparent conducting oxide (TCO) CdO and doped TCO exhibit high transparency in the visible portion of the optical spectrum. Combination of high transparency with useful electrical conductivity makes cadmium oxide technologically useful. We calculate the transport properties such as conductivity and Hall coefficient are calculated to study the effect of 1.6% doping of CdO with Sc, Y and Ti. Amongst the transparent conducting oxides, CdO has very low electrical resistivity. The most important charge transport property, the electrical conductivity as a function of temperature is calculated using Eq. (13). The calculated conductivity values at room temperature for pure and Sc-, Y- and Ti-doped CdO are presented in Table 1. Yttrium doped CdO shows maximum conductivity, whereas Ti-doped CdO shows anomalous behaviour. The electrical conductivity of CdO is, thus, enhanced due to the substitution of 1.6% atom of dopant ion with ionic radii smaller than Cd ion. The increase in electrical conductivity is due to increase in the carrier concentration. The substitution of Sc^{3+}, Y^{3+} or Ti^{4+} ions for Cd^{2+} ion in the CdO structure, results in one or more free electrons that contribute to the electrical conductivity. The FP-LAPW calculated conductivity of 3.96×10^4 $(\Omega m)^{-1}$ shows good agreement with the measured value 5.4×10^4 $(\Omega m)^{-1}$ for CdO at room temperature[6]. Measurements for doped-CdO samples are not available for comparison.

The Hall coefficients can also be calculated using Eq. (14). The calculation of the Hall coefficient depends on the second derivatives of the bands, is an important test for the theoretical method. The Sc-, Y- and Ti-doped CdO exhibit *n*-type conductivity as determined from the negative Hall coefficients as presented is in Table 1. The Hall coefficient of CdO is enhanced due to the substitution of 1.6% atom of dopant ion. However, Hall coefficient measurements for doped-CdO samples are not available for comparison.

4 Conclusions

In this paper, the electronic and optical properties of pure and Sc-, Y-, Ti-doped CdO compound using the FP-LAPW method are presented. The density of states of CdO is modified due to additional d-states of dopant ion in the conduction region. The doped compounds show enhanced 80-85% transmittance in the optical region. The optical absorption profiles clearly indicate that the doped-TCO has possibility of greater multiple direct and indirect inter band transitions compared to pure CdO. Thus, doping of CdO with metallic ions of smaller radius than that of Cd^{2+} like Sc, Y, Ti etc. increases the optical gap, improves its transmittance and electrical conductivity. Calculation with different doping concentrations and ionic radii are urgently required in order to improve the optical response.

Acknowledgement

We are thankful for financial assistance provided by Defence Research Development Organization (DRDO), New Delhi. We acknowledge with thanks to Prof P Blaha and team for providing Wien2k package.

References

1 Dau Y, Egdell R G, Law D S L, Harrison N M & Searle B G, *J Phys Condens Matter,* 10 (1998) 8447.
2 Piper L F J, Demasi A, Smith K E, Schleife A, Fuchs F, Bechstedt F, Zuniga-Perez J & Sanjose V M, *Phys Rev B*, 77 (2008) 125204
3 Choudhary G, Rayker V, Tiwari S, Dashora A & Ahuja B L, *Phys Status Solidi B,* (2010) 1.
4 Jaffe J E, Pandey R & Kunz A B, *Phys Rev* B, 43 (1991) 17.
5 Schleife A, Rodl C, Fuchs F, Furthmuller J & Bechstedt F, *Phys Rev B*, 80 (2009) 035112.
6 Rusu RS & Rusu G J, *J Opto Elec Adv Mat*, 7 (2005) 82.
7 Dakhel A A, *Optical Mater,* 31 (2009) 691.
8 Dakhel A A, *J Alloys & Compd,* 475 (2009) 51.
9 Jin S, Yang Y, Medvedeva J E, Wang L, Li S, Cortes N, Ireland J R, Metz A W, Ni J, Hersam M C, Freeman A J & Marks T J, *Chem Matter*, 20 (2008) 220.
10 Medvedeva J E & Freeman A J, *Europhys Lett,* 69 (2005) 583.
11 Yang Y, Jin S, Medvedeva J E, Ireland J R, Metz A W, Ni J, Hersam M C, Freeman A J & Marks T J, *J Am Chem Soc*, 127 (2005) 8796.
12 Jin S, Yang Y, Medvedeva J E, Ireland J R, Metz A W, Ni J, Kannewurf C R, Freeman A J & Marks T J, *J Am Chem Soc*, 126 (2004) 13787.
13 Medvedeva J E, *Appl Phys A*, 89 (2007) 43.
14 Medvedeva J E, *EPL,* 78 (2007) 57004.
15 Dou Y, Fishlock T, Egdell R G, Law D S L & Beamson G, *Phys Rev B,* 55 (1997) R13381.
16 Saha B, Thapa R & Chattopadhyay K K, *Solid State Commun*, 145 (2008) 33.
17 Gupta R K, Ghosh K, Patel R & Kahol P K, *Appl Surface Sci*, 255 (2009) 6252.
18 Blaha P, Schwarz K, Madsen G K H, Kvasnicka D & Luitz J, *WIEN2k,* Vienna University of Technology, Vienna, Austria (2001).
19 Wu Z & Cohen R E, *Phys Rev B*, 72 (2006) 235116.
20 Blochl P E, Jepsen O & Andersen O K, *Phys Rev* B, 49 (1994) 16223.
21 Amrosch-Draxl C & Sofo J O*, Comput Phys Commun,* 175 (2006)1.
22 Madsen G K H & Singh J D*, Comp Phys Comm*, 175 (2006) 67.
23 Landolt-Börnstein- Group III Condensed Matter, Volume 41 B: II-VI & I-VII Compound, Edited by O Madelung, U Rössler & M Schulz
24 Burstien E*, Phys Rev*, 93 (1954) 632.
25 Moss I S, *Proc Phys Soc Lond B*, 67 (1954) 775.
26 Yang Z, Zhong W, Yin Y, Du X, Deng Y, Au C & Du Y, *Nanoscale Res Lett*, 5 (2010) 961.